Proc. Natl. Acad. Sci. USA
Vol. 80, pp. 2235–2239, April 1983
Biophysics

Nanosecond absorption spectroscopy of hemoglobin: Elementary processes in kinetic cooperativity

(photodissociation/geminate recombination/quaternary structure/tertiary structure/singular value decomposition)

JAMES HOFRICHTER, JOSEPH H. SOMMER, ERIC R. HENRY, AND WILLIAM A. EATON

Laboratory of Chemical Physics, National Institute of Arthritis, Diabetes, Digestive and Kidney Diseases, National Institutes of Health, Bethesda, Maryland 20205

Communicated by Robin M. Hochstrasser, January 7, 1983

ABSTRACT **A nanosecond absorption spectrometer has been used to measure the optical spectra of hemoglobin between 3 ns and 100 ms after photolysis of the CO complex. The data from a single experiment comprise a surface, defined by the time-ordered set of 50–100 spectra. Singular value decomposition is used to represent the observed spectra in terms of a minimal set of basis spectra and the time course of their amplitudes. Both CO rebinding and conformational changes are found to be multiphasic. Prior to the quaternary structural change, two relaxations are observed that are assigned to geminate recombination followed by a tertiary structural change. These relaxations are interpreted in terms of a kinetic model that points out their potential role in kinetic cooperativity. The rapid escape of CO from the heme pocket compared with the rate of rebinding observed for both *R* and *T* quaternary states shows that the quaternary structure controls the overall dissociation rate by changing the rate at which the Fe—CO bond is broken. A comparable description of the control of the overall association rates must await a more complete experimental description of the kinetics of the quaternary *T* state.**

Beginning with the work of Gibson (1), experiments on the photolysis of the CO complex of Hb have played a central role in investigations of the mechanism of cooperative ligand binding (2). Hopfield *et al.* (3) proposed that the major features of the bimolecular recombination kinetics could be rationalized by a two-state allosteric model in which the *R* and *T* quaternary structures are in equilibrium. Subsequent studies have focused on measuring the rate of the quaternary structural transition (4–6). Recent improvements in time resolution have introduced new dimensions to the binding mechanism. Transient absorption spectroscopy using 10-ps laser pulses at room temperature showed no evidence of CO rebinding in <1 ns (7, 8). Significant recombination of CO was observed, however, at 50–100 ns in experiments using 10- to 30-ns laser pulses (9–13). This has been interpreted as the rebinding of photodissociated CO that has not yet escaped from the protein into the solvent and is called "geminate" recombination (9–13). At later times, both optical absorption and resonance Raman spectra of the deoxy hemes showed spectral changes in 0.5–5 μs, which have been interpreted as resulting from tertiary conformational changes of the globin (14, 15).

No kinetic model has been formulated that relates geminate rebinding to heme stereochemical and globin conformational changes or to the overall thermal ligand dissociation and binding reactions. A major objective of the present study is to make this connection. Our approach has been to measure precise optical absorption spectra over a wide range of time (from ≈3 ns to 100 ms) following photolysis of HbCO. The results suggest a kinetic model that gives additional insight into the nature of the elementary processes responsible for cooperativity.

The publication costs of this article were defrayed in part by page charge payment. This article must therefore be hereby marked "*advertisement*" in accordance with 18 U. S. C. §1734 solely to indicate this fact.

MATERIALS AND METHODS

Human HbO_2 A was purified by column chromatography of a freshly prepared lysate on DEAE-cellulose (Whatman DE-52), dialyzed against 0.1 M potassium phosphate (pH 7.0), equilibrated with CO, and diluted to a final concentration of 0.125 mM in the same buffer containing CO and 0.01 M sodium dithionite.

Transient difference absorption spectra were measured at room temperature with a spectrometer that uses two neodymium:YAG lasers producing 10-ns pulses (full-width at half-maximum), a spectrograph, and an optical multichannel analyzer system. The 532-nm harmonic of one laser (DCR-1A, Quanta Ray, Mountain View, CA) excites the sample while the 355-nm harmonic of the second laser excites spontaneous fluorescence from a dye that is used to probe the sample. The dye (1.5 mM stilbene 420 in methanol; Exciton Chemical, Dayton, OH) provides a reproducible broadband source with emission in the range 390–475 nm. Because the population of the excited state of the dye is rapidly depleted by stimulated emission, the intensity of the dye pulse closely follows the time course of the laser pulse. The time delay between firing the two lasers is controlled by a specially constructed timing circuit and a Hewlett-Packard 5359A time synthesizer. Measurement of the actual time delay is achieved with a pair of fast photodiodes (Hewlett-Packard 5082-4220) and a Hewlett-Packard 5335A universal counter.

The optical configuration is that of a split-beam difference absorption spectrometer. The dye emission is focused inside the excited region of the sample contained in a cuvette having a 0.34-mm path length (EPR aqueous cell, WG-814, Wilmad Glass, Buena, NJ), imaged onto the 100-μm-wide entrance slit of a 0.25-m spectrograph with a 600 groove per mm holographic grating (M-20 J-Y Optical Systems, Metuchen, NJ), and dispersed onto the face of a silicon vidicon tube (1256E, Princeton Applied Research, Princeton, NJ). The reference beam is generated by focusing an image of the dye source just below the excited region of the dye cell. This beam is, in turn, focused onto an unexcited region of the sample and dispersed onto an adjacent region of the vidicon tube using the optics that focus the sample beam.

In a typical experiment, averaged difference spectra were measured at 50–100 different time delays between firing the photolysis and probe lasers. The measured spectra were processed by singular value decomposition (SVD) (16, 17) to determine the minimum set of basis spectra necessary to describe the data. This procedure also produced the time dependence of each of these basis spectra.

Abbreviation: SVD, singular value decomposition.

To test the accuracy of our spectrometer and to ensure that the laser pulses do not produce any photochemistry other than CO dissociation, we carried out a series of measurements on the photolysis of MbCO. These experiments, discussed in detail elsewhere (18), showed that the spectrum of the photoproduct 15 ns after photolysis is identical to that of equilibrium deoxymyoglobin. In Mb, ≈4% of the deoxyhemes produced by photodissociation rebind CO in a single geminate process and the remaining 96% rebind in a single bimolecular process (18).

RESULTS

Transient spectra of Hb measured after photolysis of HbCO are shown in Fig. 1. The time at which the maximum amplitude was observed was taken as zero time for all of the subsequent analysis. SVD of 103 spectra between 0 and 85 ms yields three significant basis spectra (Fig. 2). The basis spectrum with by far the largest singular value (17.3) is a Hb−HbCO type difference spectrum. The basis spectrum with the next largest singular value (1.27) has almost no feature at the HbCO peak and is most readily interpreted as arising from a Hb spectral change. The third significant basis spectrum has a very small singular value (0.082) and was chosen based on the autocorrelation of its time dependence and its spectral shape. The time course of each of the three basis spectra could be well represented by five exponential relaxations, where the relaxation times are the same for all three basis spectra. These $1/e$ times, together with the amplitude changes for the basis spectra associated with each of the five relaxations, constitute a highly condensed but accurate representation of the 103 measured spectra.

The most straightforward part of analyzing the results is to generate progress curves for the ligand binding kinetics. SVD shows that basis spectrum 2 (Fig. 2*a*) has zero amplitude at 438 nm; i.e., 438 nm is a near isosbestic point for the Hb spectral change. Basis spectrum 3 (Fig. 2*b*) has a finite amplitude at 438 nm, but it is only 0.3% of that of basis spectrum 1 after scaling for their relative singular values. Thus, the A at 438 nm or, more accurately, the amplitude of basis spectrum 1, is directly proportional to the fraction of unliganded hemes. Ligand binding kinetic progress curves for four different photolysis experiments are shown in Fig. 3.

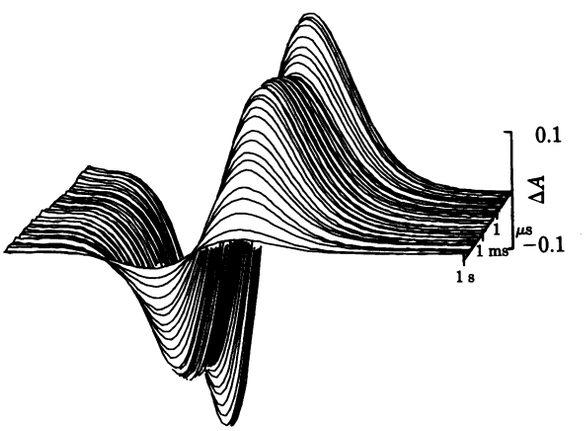

FIG. 1. Spectra after photolysis of HbCO. A representative subset of the transient difference spectra collected for sample b, in which 100% saturated HbCO was fully photolyzed (90%) at 0.1 atm CO pressure (1 atm = 101.3 kPa) is shown. Each curve represents the difference in A between the deoxy photoproduct and the HbCO reference on the vertical (y) axis as a function of wavelength (x). The logarithm of the time is plotted on the z axis with the earliest times in the background. The data span eight decades of time (1 ns to 0.1 s) with five spectra per decade. The sample A at the CO peak (419 nm) was 0.81 and the peak (430 nm) A in a fully deoxygenated reference spectrum was 0.575.

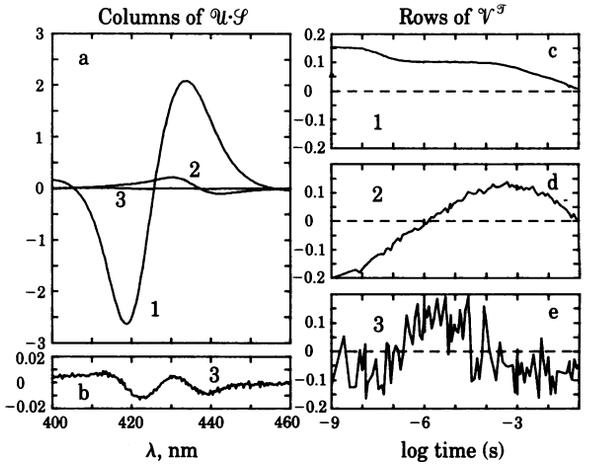

FIG. 2. SVD of observed spectra. The SVD of $\mathcal{A}$ is defined as $\mathcal{A} = \mathcal{U}\mathcal{S}\mathcal{V}^{\mathcal{T}}$ (16, 17), where $\mathcal{A}$ is the $m \times n$ matrix of spectra measured at n different time delays between photolysis and probe pulses and each of the n columns contains absorbance values at m wavelengths; $\mathcal{U}$ is an $m \times n$ matrix in which the columns of $\mathcal{U}$ are an orthonormal set of m-dimensional vectors, which we call the basis spectra; $\mathcal{S}$ is an $n \times n$ diagonal matrix with all nonnegative elements, called the singular values of $\mathcal{A}$; and $\mathcal{V}$ is an $n \times n$ unitary matrix in which the rows of $\mathcal{V}^{\mathcal{T}}$ (columns of $\mathcal{V}$) are the time courses of the amplitudes of each of these basis spectra. (*a*) The three basis spectra obtained by SVD from the 103 spectra observed in the experiment shown in Fig. 1. The basis spectra are scaled by their singular values, $S_1 = 17.3$, $S_2 = 1.27$, $S_3 = 0.082$, to display their relative contributions to the observed data. (*b*) Basis spectrum 3 displayed on an expanded scale. (*c–e*) Normalized time dependences of the three basis spectra. The increasing noise in each of the successive components results from the decreased amplitude of each basis spectrum in the observed spectra. In fitting the time dependence, these data were weighted by the singular value associated with each basis spectrum.

It is much more difficult to generate the spectra and progress curves for the deoxy intermediates in ligand binding. The difficulty arises because the spectra of hemes in the same ligation

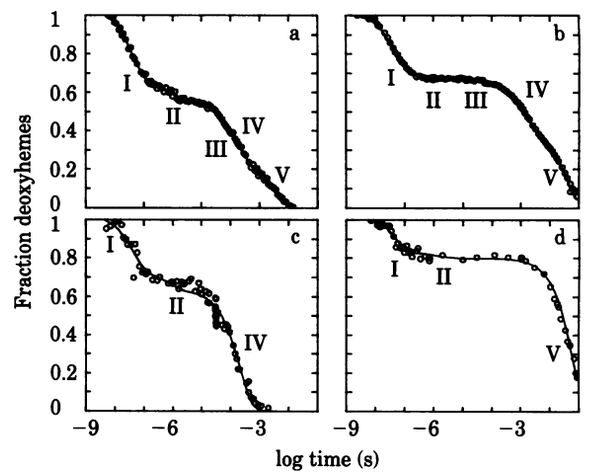

FIG. 3. CO recombination kinetics. The kinetics of CO rebinding to photolyzed HbCO are shown. (*a*) 1.0 atm CO, 100% saturation, full photolysis. (*b*) 0.1 atm CO, 100% saturation, full photolysis. (*c*) 1.0 atm CO, 100% saturation, 22% photolysis. (*d*) 3×10^{-6} atm CO, 10% saturation, full photolysis. The fraction of deoxyhemes was obtained by dividing the amplitude of the first SVD basis spectrum at each time by the amplitude at the peak of photolysis. The lines through the data show the fit to the amplitude of the first basis spectrum obtained from the simultaneous least-squares fit to the time dependence of all of the significant basis spectra obtained from the SVD analysis of each data set.

state are very similar (19, 20). The resolution of three significant basis spectra by SVD permits determination of the spectra and time courses for three spectrally distinct deoxy intermediates. One of the three spectra can be obtained by making the plausible assumption that the zero time spectrum is that of a single species. The second can be assigned to completely unliganded deoxyhemoglobin (*T*-state Hb) since the measured spectrum before the fifth and last relaxation is identical to a Hb−HbCO static difference spectrum. The time course of basis spectrum 3 (Fig. 2*e*) indicates that there is a species that appears subsequent to photolysis and disappears prior to completion of ligand binding. If we assume that this species is pure before the third of the five relaxations, the spectra, $D_k(\lambda)$, k = 1, 3, 5, of the three species existing prior to the first, third, and fifth relaxations can be calculated as linear combinations of the three basis spectra, using coefficients obtained from the least-squares fits to the time dependence of the three basis spectra. The time dependence of the sample composition in terms of the three species having these spectra can also be calculated directly from the SVD results. The spectra, $D_k(\lambda)$, the (double) difference spectra between them, and the time courses of the species with these spectra are shown in Fig. 4.

The transient spectra of experiments a and c can also be constructed from linear combinations of the species spectra $D_k(\lambda)$. In experiment a, the spectra prior to the first, third, and fifth relaxations were indistinguishable from $D_1(\lambda)$, $D_3(\lambda)$, and $D_5(\lambda)$. In experiment c, the initial and final spectra were the same as $D_1(\lambda)$ and $D_3(\lambda)$. For the 10% saturated sample (d), there are three spectral relaxations. The spectrum preceding the third relaxation is the same as $D_5(\lambda)$, while the spectra preceding the first and second relaxations are different from $D_1(\lambda)$ or $D_3(\lambda)$.

The results of the data analysis are summarized in Table 1, which gives, for each relaxation, the $1/e$ time, the fractional change in saturation with CO, and the fractional change in the concentration of the species with spectrum $D_k(\lambda)$. By comparing the fractional change in CO saturation with the fractional change in species concentrations, one can ascertain whether the primary change in the sample composition is due to CO binding, conversion to another spectrally distinct species without change in CO saturation, or simultaneous CO recombination and structural change.

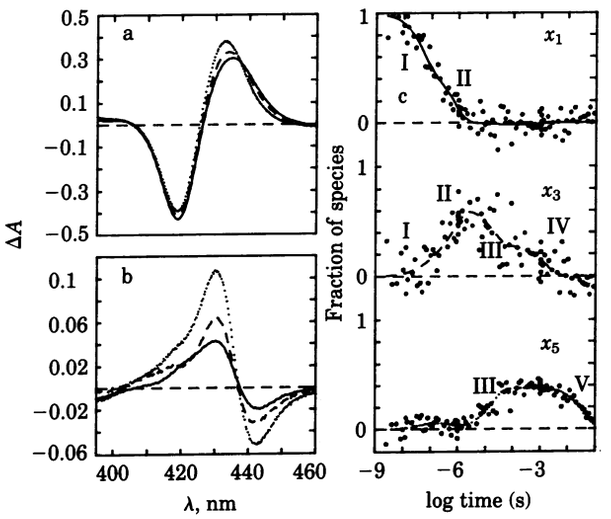

FIG. 4. Spectra and time evolution of deoxy Hb intermediates. (*a*) Normalized difference spectra: deoxy photoproducts observed in experiment b vs. HbCO. —, Initial deoxy photoproduct observed at 10 ns and denoted as $D_1(\lambda)$; ···, last deoxy species to rebind CO, denoted as $D_5(\lambda)$; ---, deoxy species maximally formed at 3 μs and denoted as $D_3(\lambda)$. (*b*) Expanded difference spectra: ···, $D_5(\lambda) - D_1(\lambda)$; ---, $D_5(\lambda) - D_3(\lambda)$; —, $D_3(\lambda) - D_1(\lambda)$. (*c*) Composition of the photolyzed sample represented in terms of the three deoxy species having the difference spectra $D_1(\lambda)$, $D_3(\lambda)$, and $D_5(\lambda)$ shown in *a*. The curves through the data in *c* are calculated from the exponential fits to the time dependence of the three SVD basis spectra given in Table 1.

Table 1. Relaxation times and amplitude changes for ligand rebinding and spectral species

Relaxation	I	II	III	IV	V
		Experiment a			
$1/e$ time	40 ns	0.83 μs	20 μs	190 μs	3.8 ms
Δy	0.37	0.09	0.03	0.29	0.22
Δx_1	−0.51	−0.49	0.11	−0.11	0
Δx_3	0.05	0.49	−0.47	−0.07	0
Δx_5	0.09	−0.09	0.33	−0.12	−0.22
		Experiment b			
$1/e$ time	50 ns	0.71 μs	18 μs	1.5 ms	40 ms
Δy	0.33	0.02	0.01	0.25	0.39
Δx_1	−0.50	−0.50	−0.02	0.02	0
Δx_3	0.10	0.54	−0.36	−0.29	0
Δx_5	0.07	−0.07	0.37	0.02	−0.39
		Experiment c			
$1/e$ time	44 ns	0.91 μs	—	200 μs	—
Δy	0.30	0.09	—	0.61	—
Δx_1	−0.47	−0.54	—	0	—
Δx_3	0.17	0.45	—	−0.61	—
Δx_5	0	0	—	0	—
		Experiment d			
$1/e$ time	45 ns	1.4 μs	—	—	60 ms
Δy	0.21	0.03	—	—	0.76
$\Delta x_1'$	−0.54	−0.46	—	—	0
Δx_5	0.33	0.43	—	—	−0.76

Experiments a–d are described in Fig. 3. Δy = change in fractional saturation of ligand and Δx_k = fractional change in the population of species with spectrum D_k (λ) (Fig. 4) associated with each relaxation. The data have been normalized to the number of deoxyhemes initially photolyzed. The average relative error in the relaxation times is 20% and the average absolute errors in Δy and Δx_k are 0.02 and 0.1, respectively.

DISCUSSION

A principal objective of our study of transient spectra and kinetics is to determine the origin of the difference in rates for the first and last ligands in the overall binding and dissociation reaction of Hb with CO. One can ask whether the change in quaternary structure alters the rates of entrance and exit of the ligand to and from the heme pocket, the rates of binding and dissociation at the heme, or the rates of tertiary conformational changes that are not simultaneous with either of these processes. To investigate these questions, the individual processes must be identified so that their rates can be compared for the two quaternary structures. The present work is a first step toward this goal. It includes four experiments. In experiment a, 100% saturated HbCO was fully photolyzed at a CO pressure of 1 atm. In experiment b, 100% saturated HbCO was fully photolyzed at a CO pressure of 0.1 atm to distinguish first- and second-order processes. In experiment c, fully saturated HbCO was only partially (20%) photolyzed. This experiment was designed to measure the bimolecular binding rate for *R*-state hemoglobin and to investigate spectral changes in molecules that should not undergo the $R \rightarrow T$ quaternary change. In experiment d, the hemes were 10% saturated with CO and were fully photolyzed. This experiment was performed to examine the properties of Hb with a large fraction of the liganded hemes in molecules having the *T*-quaternary structure.

The $1/e$ times and spectral properties of the observed re-

laxations are summarized in Table 1. Our problem is to assign these relaxations to elementary processes. To simplify the discussion, we use the framework of the two-state allosteric model for interpreting the relaxations (4). We begin by discussing the data at times greater than ≈10 μs. This time regime was investigated to locate the $R \rightarrow T$ transition and to characterize the four samples in terms of the overall combination reaction. We then discuss the shorter time regime in which geminate recombination and spectral changes assigned to tertiary conformational changes are observed. Finally, the assignments in the geminate regime are summarized by a kinetic model that is then used in discussing the elementary processes responsible for kinetic cooperativity.

The quaternary structural change and bimolecular recombination

In discussing the bimolecular recombination kinetics, the most straightforward experiment is c in which ≈20% of the hemes were photolyzed. In this sample, CO recombines in a bimolecular reaction to molecules having an average saturation of ≈86%, and the rebinding is well fitted with a single exponential function yielding a bimolecular rate constant of 6×10^6 $mol^{-1} \cdot s^{-1}$ (Fig. 3*c*), in agreement with previously reported values for *R*-state Hb (4, 21). Furthermore, the spectrum of the deoxy species is very similar to the spectrum of so-called "fast-reacting" Hb, also known as Hb* (1, 4). The spectrum of Hb* has been assigned to deoxyhemoglobin in the *R*-quaternary structure (4, 19), the arrangement of subunits found in the fully liganded molecule (22). Bimolecular recombination to the initially 10% saturated sample of experiment d is also well fitted with a single exponential function (Fig. 3*d*), yielding a bimolecular rate constant of 1.3×10^5 $mol^{-1} \cdot s^{-1}$, in good agreement with reported values for the binding of the first ligand to completely deoxy (*T*-state) Hb (4, 23). Again the spectra and kinetic data are consistent, the spectrum of the recombining species being indistinguishable from that of *T*-state Hb (Fig. 4).

The results for the 100% saturated completely photolyzed samples (a and b) are more complex, with three distinct relaxations observed for each sample (Table 1, Figs. 3 and 4). The first of these, relaxation III occurring at ≈20 μs, is primarily a spectral change with little or no ligand recombination. This relaxation is assigned to the $R \rightarrow T$ quaternary transition, because a corresponding spectral change is absent in the partially photolyzed sample (c). The spectral data support this assignment; both the shape and absolute amplitude of the spectral change (Fig. 4*b*) are similar to the well-known $T - R$ difference spectrum (4, 19). Since the recombination data require that some liganded molecules switch from *R* to *T*, 5×10^4 s^{-1} must be considered a lower limit for the $R_0 \rightarrow T_0$ rate constant (cf. refs. 5 and 6). The identification of the $R \rightarrow T$ transition is critical to the assignment of earlier spectral changes as pure tertiary structural changes (see below).

Relaxation IV in samples a and b involves both an $R \rightarrow T$ spectral change and ligand rebinding, while relaxation V results only from ligand rebinding. The amplitudes and $1/e$ times for relaxations IV and V can be qualitatively explained in terms of a two-state allosteric kinetic model (3, 4). A quantitative analysis of these relaxations will be presented elsewhere.

Geminate recombination and tertiary structural changes

The spectrum of the immediate photoproduct is a new spectrum and is the same for all three *R*-state samples (a–c). The difference between this spectrum and that of *T*-state Hb is similar to the $T - R$ difference spectrum but has about twice the amplitude (Fig. 4*b*). It is not possible to make any detailed structural interpretation of this deoxyheme spectrum, since neither sufficient data to allow an empirical assignment nor an adequate theory for the origin of the Soret band shape is available.

In the three *R*-state samples, photodissociation is followed by relaxations I at 40–50 ns and II at 0.7–0.9 μs. From the CO pressure independence of the amplitude of ligand rebinding and the $1/e$ time of relaxation I in samples a and b, we conclude, in agreement with previous workers (9–13), that the CO recombination is geminate; i.e., the CO rebinds to the heme from which it was photodissociated. Since free diffusion of the photodissociated molecule in water would reduce the local concentration to well below the free CO concentration within 10 ns, this requires either that the ligand diffuse slowly inside the protein or that there be a weak nonheme binding site for CO within the protein. At present, the data on the detailed kinetic form are insufficient to distinguish between these two possibilities (12, 13). For simplicity, we shall assume that the ligand binds to a site close to the heme, the region commonly referred to as the heme pocket.

Relaxation I is also accompanied by a spectral change (Table 1) that has two possible interpretations. One is that both the geminate yield and immediate photoproduct spectra are different for the α and β subunits, so that the spectral change simply results from preferential binding to α or β subunits. The second, more likely possibility, is that it is caused by a structural change. This change is effectively simultaneous with the exit of the CO from the heme pocket and could result from collapse of the globin into the hole left by the ligand.

The final relaxation to assign in samples a–c is relaxation II, which occurs between 0.7 and 0.9 μs. This relaxation is primarily a spectral change. Because the same spectral change is observed with the same rate and amplitude in the partial photolysis experiment (c) (Table 1), in which there is both kinetic and spectroscopic evidence that there is no $R \rightarrow T$ transition, the associated structural change can be considered as a pure tertiary change. A tertiary change in this time regime has been previously proposed on the basis of transient Raman (14) and single-wavelength absorption studies (15). There is a small change in fractional saturation associated with relaxation II, suggesting geminate rebinding from a second nonheme binding site in the globin (13). The limited data presented here, however, hint that the small change in fractional saturation is dependent on the CO pressure. If confirmed by more detailed studies, this observation would indicate that the rebinding associated with relaxation II is bimolecular with a very high rate (1×10^8 $mol^{-1} \cdot s^{-1}$). The molecule existing prior to relaxation II might then be "superfast reacting" Hb.

The interpretation of relaxations I and II for the 10% saturated sample (d) is complicated by the lack of experimental information on the distribution of molecular species prior to photolysis. When the two-state allosteric parameters $L = 60{,}000$ and $c = 0.01$ (24) are used, 65% of the liganded hemes are predicted to be in singly or doubly liganded *T*-state molecules and 35% are in triply or quadruply liganded *R*-state molecules. Even though the spectra and kinetics of this sample are expected to be those of a mixture of *R*- and *T*-state Hb, we can make several qualitative conclusions concerning *T*-state properties. First, the spectrum of the immediate *T*-state photoproduct is significantly different from the spectrum of the immediate *R*-state photoproduct, in that it is closer to an equilibrium *T*-state spectrum. Second, the *T*-state geminate yield must be less than the observed value for this sample of 21% (Table 1), which is about two-thirds that observed for the *R* state. Finally, there is also a *T*-state tertiary structural change occurring before 1 μs, but we cannot determine its relaxation time more precisely.

Kinetic cooperativity

The interpretations discussed above for *R*-state Hb can be summarized by a four-species kinetic model:

$$\mathrm{RrCO} \underset{k_{21}}{\overset{k_{12}}{\rightleftharpoons}} [\mathrm{Rr{\cdot}CO} \underset{k_{32}}{\overset{k_{23}}{\rightleftharpoons}} \mathrm{Rr} + \mathrm{CO} \underset{k_{43}}{\overset{k_{34}}{\rightleftharpoons}} \mathrm{Rt} + \mathrm{CO}.$$

According to this model, photolysis populates Rr·CO in which the CO is still in the heme pocket. Rr·CO disappears in relaxation I because the photodissociated CO either rebinds to the heme or escapes from the heme pocket into the solvent, allowing the globin to relax to yield Rr. Rr disappears in relaxation II, primarily by undergoing a tertiary conformational change to form Rt (= Hb*), although CO rebinds via Rr·CO to the hemes of a small fraction in a superfast bimolecular process. From least-squares fits to the ligand binding curves, the rate constants for this model are $k_{21} = 6 \times 10^6 s^{-1}$, $k_{23} = 10 \times 10^6 s^{-1}$, $k_{32} = 3 \times 10^8$ mol^{-1}·s^{-1}, $k_{34} = 1 \times 10^6 s^{-1}$. The proposed model does not provide a unique explanation of the available data, but it is the simplest kinetic scheme consistent with the present results.

If we assume that the same basic mechanism exists for *T*-state Hb, we can use this model to examine the roles that these rapid processes play in cooperative ligand binding. In the reaction of Hb with CO, the higher affinity of the *R* state compared with the *T* state results from an increase in the overall association rate and a decrease in the overall dissociation rate. In the case of the reaction with O_2, the increase in affinity results mainly from a decrease in the overall dissociation rate. Szabo (25) has used transition-state theory to show that the mechanism of cooperativity could be very similar for CO and O_2 in spite of their different kinetic behavior. In his analysis, all of the cooperativity arises from the difference between the *R* and *T* states in the free energy required to change the conformation of the globin on the proximal side of the heme; this conformational change is simultaneous with the bond formation and breaking steps, and is caused by the iron motion relative to the heme plane in these steps, as originally proposed by Hoard and Perutz (22). Szabo assumed that steric effects on the distal side of the heme (22, 26) and the rates of other processes, such as additional conformational changes or access of the ligand to the heme pocket, are the same for the *R* and *T* states. These assumptions can be tested by evaluating the rate constants of our kinetic model for both *R*- and *T*-state Hb, since the difference in overall rates is predicted to appear exclusively in k_{12} and k_{21}.

The only available data suggest that the overall CO dissociation rates for *R*- and *T*-state Hb differ by a factor of ≈ 10 [$^R k_{off} = 0.009\ s^{-1}$, $^T k_{off} = 0.09\ s^{-1}$ (27)]. According to our model, the rate constant for the overall dissociation of CO at zero free [CO], k_{off}, is related to the thermal bond-breaking rate constant, k_{12}, in the steady-state approximation, by

$$k_{off} = k_{12}(1 - \phi),$$

where the geminate yield, ϕ, is $k_{21}/(k_{21} + k_{23})$. For *R*-state Hb, $1 - \phi = 0.6$–0.7 while, for *T*-state Hb, $1 - \phi = 0.8$–1. This result suggests that the difference in the overall dissociation rates for *R*- and *T*-state Hb results primarily from the bond-breaking rate constant, k_{12}, since the ratio of the values of $(1 - \phi)$ for the *T* and *R* states is <1.7.

Kinetic cooperativity is much larger for the overall combination reaction with $^R k_{on}/^T k_{on} = 50$ (Table 1). In our model, k_{on} is related to the rate constants for the elementary processes in the steady-state approximation by

$$k_{on} = \frac{k_{32}k_{43}\phi}{k_{34} + k_{43} + k_{32}\phi[\mathrm{CO}]} \approx k_{32}\frac{k_{43}}{k_{34}}\phi.$$

In contrast to the overall dissociation rate, the overall association rate depends on ϕ, the equilibrium constant (k_{43}/k_{34}) for the tertiary conformational change, and the rate of entry of CO into the heme pocket (k_{32}). If all of the decrease in k_{on} for the *T* state results from a decreased binding rate at the heme (k_{21}), the model predicts a ϕ value of only 0.007 and a $1/e$ time for relaxation I of 100 ns after photolysis of pure *T*-state HbCO. Although a value of ϕ near zero is suggested from measurements of the apparent photochemical quantum yield using microsecond lasers (28), a test of the prediction requires accurate measurements of both the geminate yield and the relaxation time for the *T* state.

We thank Robin M. Hochstrasser for encouraging us to develop a laser spectrometer and Attila Szabo for many rewarding discussions on the cooperativity problem.

1. Gibson, Q. H. (1959) *Biochem. J.* **71**, 293–303.
2. Antonini, E. & Brunori, M. (1971) *Hemoglobin and Myoglobin in Their Reaction with Ligands* (North-Holland, Amsterdam).
3. Hopfield, J. J., Shulman, R. G. & Ogawa, S. (1971) *J. Mol. Biol.* **61**, 425–443.
4. Sawicki, C. A. & Gibson, Q. H. (1976) *J. Biol. Chem.* **251**, 1533–1542.
5. Ferrone, F. A. & Hopfield, J. J. (1976) *Proc. Natl. Acad. Sci. USA* **73**, 4497–4501.
6. Cho, K. C. & Hopfield, J. J. (1979) *Biochemistry* **18**, 5826–5833.
7. Greene, B. I., Hochstrasser, R. M., Weisman, R. B. & Eaton, W. A. (1978) *Proc. Natl. Acad. Sci. USA* **75**, 5255–5259.
8. Chernoff, D. A., Hochstrasser, R. M. & Steele, A. W. (1980) *Proc. Natl. Acad. Sci. USA* **77**, 5606–5610.
9. Duddell, D. A., Morris, R. J. & Richards, J. T. (1979) *J. Chem. Soc. Chem. Commun.*, 75–76.
10. Alpert, B., El Mohsni, S., Lindqvist, L. & Tfibel, F. (1979) *Chem. Phys. Lett.* **64**, 11–16.
11. Friedman, J. M. & Lyons, K. B. (1980) *Nature (London)* **284**, 570–573.
12. Lindqvist, L., El Mohsni, S., Tfibel, F., Alpert, B. & Andre, J. C. (1981) *Chem. Phys. Lett.* **79**, 525–528.
13. Catterall, R., Duddell, D. A., Morris, R. J. & Richards, J. T. (1982) *Biochim. Biophys. Acta* **705**, 256–263.
14. Lyons, K. B. & Friedman, J. M. (1982) in *Hemoglobin and Oxygen Binding*, eds. Ho, C., Eaton, W. A., Collman, J. P., Gibson, Q. H., Leigh, J. S., Margoliash, E., Moffat, J. K. & Scheidt, W. R. (Elsevier/North-Holland, Amsterdam), pp. 333–338.
15. Lindqvist, L., El Mohsni, S., Tfibel, F. & Alpert, B. (1980) *Nature (London)* **288**, 729–730.
16. Shrager, R. I. & Hendler, R. W. (1982) *Anal. Chem.* **54**, 1147–1152.
17. Golub, G. H. & Reinsch, C. (1970) *Numer. Math.* **14**, 403–420.
18. Henry, E. R., Sommer, J. H., Hofrichter, J. & Eaton, W. A. (1983) *J. Mol. Biol.*, in press.
19. Perutz, M. F., Ladner, J. E., Simon, S. R. & Ho, C. (1974) *Biochemistry* **13**, 2163–2172.
20. Sugita, Y. (1975) *J. Biol. Chem.* **250**, 1251–1256.
21. DeYoung, A., Pennelly, R. R., Tan-Wilson, A. L. & Noble, R. W. (1976) *J. Biol. Chem.* **251**, 6692–6698.
22. Perutz, M. F. (1970) *Nature (London)* **228**, 726–734.
23. Olson, J. S. (1981) *Methods Enzymol.* **76**, 631–651.
24. Sunshine, H. R., Hofrichter, J., Ferrone, F. A. & Eaton, W. A. (1982) *J. Mol. Biol.* **158**, 251–273.
25. Szabo, A. (1978) *Proc. Natl. Acad. Sci. USA* **75**, 2108–2111.
26. Moffat, K., Deatherage, J. F. & Seybert, D. W. (1979) *Science* **206**, 1035–1042.
27. Sharma, V. S., Schmidt, M. R. & Ranney, H. M. (1976) *J. Biol. Chem.* **251**, 4267–4272.
28. Sawicki, C. A. & Gibson, Q. H. (1979) *J. Biol. Chem.* **254**, 4058–4062.